The Rearrangement of 2,2-Diphenyl-1-[(*E*)-2-phenylethenyl]cyclopropane to 3,4,4-Triphenylcyclopent-1-ene: a DFT Analysis

by **Willi Sicking**[a]), **Reiner Sustmann***[a]), **Johann Mulzer**[b]), and **Rolf Huisgen**[c])

[a]) Institut für Organische Chemie, Universität Duisburg–Essen, Campus Essen, D-45117 Essen
[b]) Institut für Organische Chemie der Universität Wien, Währinger Strasse 38, A-1090 Wien
[c]) Department Chemie der Ludwig-Maximilians Universität, Butenandt-Strasse 5 – 13, D-81377 München

Dedicated to *Paul von Ragué Schleyer*, friend and mentor, on the occasion of his 80th birthday

A computational study on the rearrangement of 2,2-diphenyl-1-[(*E*)-2-phenylethenyl]cyclopropane (**1**) is presented, using density functional theory (DFT), (U)B3LYP with the 6-31G* basis set (DFT1) and (U)M05-2X with the 6-311 + G** basis set (DFT2). In agreement with a biradical character of the transition structure (TS) or intermediate, the potential-energy hypersurface is lowered by the influence of three conjugated Ph groups. Surprisingly, two conformations of the geminal diphenyl group (different twist angles) induce two different minimum-energy pathways for the rearrangement. Independent of the functional used, the first hypersurface harbors true biradical intermediates, whereas the second energy surface is a flat, slightly ascending slope from the starting material to the TS. The functional (U)M05-2X with the basis set 6-311 + G** provides realistic energies which seem to be close to experiment. The activation energy for racemization of enantiomers of **1** is lower than that of rearrangement by 2.5 kcal mol^{-1}, in agreement with experiment.

1. Introduction. – The rearrangement of vinylcyclopropane and its derivatives to substituted cyclopentenes has played an important role in the development of mechanistic and theoretical organic chemistry. Ever since the discovery of this reaction, independently by *Vogel* [1], and by *Overberger* and *Borchert* [2], it has been studied experimentally and theoretically. It played a role in the presentation of the *Woodward–Hoffmann* rules [3], was recognized early as involving biradical intermediates [3 – 5], and was analyzed by quantum-chemical calculations [6][7]. A critical review on mechanistic aspects of this rearrangement was provided by *Baldwin* [8].

The reaction exhibits both aspects, that of a concerted and a stepwise mechanism. However, calculations on the potential-energy surface of the unsubstituted system display only one transition structure (TS) for rearrangement and no intermediate [6]. The potential-energy surface is rather flat and diradical in nature. The TS is a biradical which undergoes ring closure to cyclopentene. The results of *Houk*'s group closely resemble those of *Davidson* and *Gajewski* [7], who took a slightly different approach. Both studies agree on the biradical nature of the rearrangement and on the preference for the *si*-stereochemistry of rearrangement suggested by the *Woodward–Hoffmann* rules [3]. For the unsubstituted system, two more TSs, slightly (0.3 – 1.1 kcal mol^{-1})

higher in energy, were calculated; they were reached by motions deviating from the minimal-energy pathway [9]. These results suggest that dynamical calculations might be more suited for the description of the vinylcyclopropane → cyclopentene rearrangement. In fact, it has been shown by *Doubleday*, *Houk* and co-workers [10], and by *Doubleday*, *Hase* and co-worker, [11] that dynamical calculations properly describe the isomer distribution of the products from (D_3)vinylcyclopropane. Dynamical calculations [12], however, are possible only for the simplest systems, in general, for the parent molecules not carrying any substituents.

The aim of this study is to investigate the influence of multiple Ph substitution on the vinylcyclopropane → cyclopentene rearrangement. Dynamical calculations are out of reach for the molecules considered. We analyze the minimal-energy pathway (MEP) of the reaction, similar to the calculations of the parent system reported by *Houk et al.* [6]. The question is whether multiple Ph substitution will qualitatively alter the structure of the potential-energy surface. Will the energy of presumed biradicals be lowered so much that intermediates appear? What is the influence of Ph groups on the rearrangement in general? For this purpose, a thorough computational analysis of the rearrangement of 1,1-diphenyl-2-[(*E*)-2-phenylethenyl]cyclopropane (s-*gauche*-**1**) to 3,4,4-triphenylcyclopentene (*cis*-**8**) was undertaken. It included the analysis of optically active derivatives, thus allowing the study of cyclopropane isomerization in combination with the rearrangement.

The rearrangement of (1*R*,2*R*)-1-methyl-2-[(*E*)-phenylethenylcyclopropane and (1*R*,2*S*)-1-phenyl-2-[(*E*)-2-phenylethenyl]cyclopropane had been reported by *Baldwin et al.* [13][14]. In our preceding publication [15], experimental details were given for the kinetics and mechanism of rearrangement of 2-[(*E*)-2-arylethenyl]-1,1-diphenylcyclopropanes to 4-aryl-3,3-diphenylcyclopentenes.

2. Computational Methodology. – Calculations were carried out with GAUSSIAN03 [16]. Geometries were optimized by density functional calculations using the (U)B3LYP functional with the 6-31G* basis set (DFT1), and the functional (U)M05-2X with the 6-311 + G** basis set (DFT2) [17]. Reactants and products were computed with closed-shell wave functions, while open-shell wave functions were used for all other structures. TSs were characterized by one negative vibration in the *Hessian* matrix.

In the general discussion, we will mostly rely on the optimized (U)M05-2X/6-311 + G** (DFT2) energies, just quoted in the text as ΔE_{SCF}, since they proved to be closest to the relative energies expected by the experiments. The structures presented in the formulae are due to (U)M05-2X/6-311 + G** calculations, except for *trans*-**7** and *trans*-**7N**, which are B3LYP/6-31G*-optimized structures. *Tables 2 – 4* (see below) show red and blue designations and energies. The red entries concern nonstationary designations and energies (**N**), while the blue values do not fulfill the convergence criteria of GAUSSIAN03, but are energetically converged to the fourth digit. Higher precision could not be reached, there remains an uncertainty of 0.1 kcal mol^{-1}.

3. Results and Discussion. – 3.1. *Ground States of 1,1-Diphenyl-2-s*-trans-*[(*E*)-2-phenylethenyl]cyclopropane* (s-*trans*-**1**) *and* of *3,4,4-Triphenylcyclopent-1-ene* (*cis*-**8**). To compare the results of calculation with the crystal structure of the starting material,

Table 1 lists relevant bond lengths, bond angles, and dihedral angles of s-*trans*-**1T** (*Scheme 1*) and compares them with the data from the X-ray structure [15], which is characterized by the **T**-arrangement of the two Ph groups at C(2)[1]). The general agreement is a check on the reliability of the calculations.

Table 1. *Structural Parameters of 1,1-Diphenyl-2-[(*E*)-2-phenylethenyl]cyclopropane* (s-*trans*-**1T**) *According to X-Ray Measurement, and B3LYP/6-31G** (DFT1) *and M05-2X/6-311 + G*** (DFT2) *Analyses*

	X-Ray structure	Calculation by	
		DFT1	DFT2
Bond lengths[a]) [Å]			
C(2)–C(3)	1.507(2)	1.514	1.506
C(1)–C(3)	1.514(2)	1.510	1.504
C(1)–C(2)	1.547(2)	1.557	1.534
C(1)–C(4)	1.473(2)	1.474	1.472
C(4)–C(5)	1.336(2)	1.345	1.334
C(5)–C(6)	1.470(2)	1.469	1.470
C(2)–C(12)	1.507(2)	1.508	1.498
C(2)–C(18)	1.502(2)	1.513	1.503
Bond angles [°]			
C(1)–C(2)–C(3)	59.40(10)	61.96	59.31
C(1)–C(3)–C(2)	61.59(10)	61.95	61.29
C(1)–C(4)–C(5)	123.07(13)	123.57	123.78
C(4)–C(5)–C(6)	126.48(13)	127.42	125.25
C(2)–C(1)–C(3)	59.01(9)	61.95	59.40
C(3)–C(1)–C(4)	120.43(13)	120.75	119.29
C(3)–C(2)–C(12)	116.72(12)	117.24	117.72
C(12)–C(2)–C(18)	114.91(12)	116.35	116.10
Dihedral angles [°]			
C(3)C(1)–C(4)C(5)	− 150.57(14)	− 149.36	− 154.00
C(1)C(4)–C(5)C(6)	− 175.74(13)	+ 179.42	− 178.64
C(4)C(5)–C(6)C(7)	− 12.6(2)	5.69	21.21
C(3)C(2)–C(12)C(13)	60.82(17)	51.21	50.61
C(3)C(2)–C(18)C(19)	19.1(2)	28.98	31.36

[a]) Numbering of atoms according to formula **1** (**T**) exp. (X-ray).

The calculations place the Ph rings of s-*trans*-**1** at C(1) in a V-arrangement (*Scheme 1*), the energy of which is arbitrarily set to ΔG(DFT1 and DFT2) = 0.0 kcal mol^{-1}. The so called **T** or stacking arrangement of the Ph groups is one of the favorable groupings of two benzene rings due to attractive interactions between a positively polarized H-atom of one Ph CH group with the negatively charged center of a second Ph ring [18][19].

This kind of aromatic π-bonding is not a new phenomenon. A T-shaped benzene dimer as well as the sandwich type were found in the unit cell of crystalline benzene

[1]) The C-atom numbering as indicated in the formula **1** (**T**).

Scheme 1

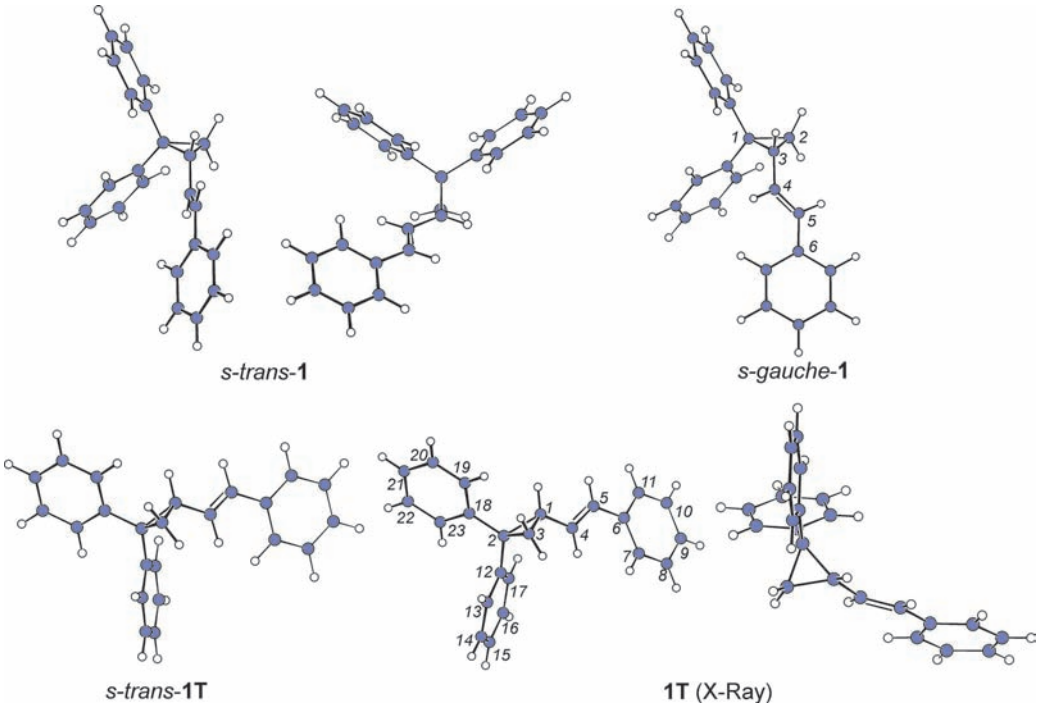

[18]. Molecular-beam studies established a dipole moment (0.6 D) in the T-dimer [20]. According to calculations (CCSD(T)aug-cc-pVDZ), the T-shaped dimer (−2.6 kcal mol^{-1}) is preferred to the sandwich type (−1.7 kcal mol^{-1}) [21].

As expected, s-*trans*-**1T** is also a minimum on the calculated potential-energy surface. A small rotational barrier ΔG of 1.6 kcal mol^{-1} (*Table 2*) separates s-*trans*-**1** and s-*trans*-**1T**. In terms of energies, the difference between *s-trans*-**1** and *s-trans*-**1T**, ΔE_{SCF}, is −0.3 kcal mol^{-1}, whereas the pertinent ΔG is +0.3 kcal mol^{-1}. Thus, the calculations seem to closely reflect the crystal situation. The preference for the **T**-arrangement of the Ph groups in the crystal could be due to packing effects. There is reason to assume that not only s-*trans*-**1T** is the favored conformation of the isolated molecule in the gas phase or in solution.

Whereas the calculated bond lengths and angles closely resemble those in the crystal, some of the dihedral angles deviate more strongly. The conformation of the (*E*)-2-phenylethenyl group displays an optimal overlap of the π-orbitals with a *Walsh* orbital of cyclopropane, as can be deduced from formula s-*trans*-**1**.

On rotating about the bond C(1)–C(4) of s-*trans*-**1** by 119°, the calculation indicates s-*gauche*-**1** as another stable conformation, the ΔG of which is by 2.5 kcal mol^{-1} higher than that of s-*trans*-**1**. A barrier of 3.5 kcal mol^{-1} in ΔE_{SCF} for TS **2** has to be passed on the way from s-*trans*-**1** to s-*gauche*-**1** (*Table 2*). Due to the insufficient convergence, ΔG

Table 2. *Energies of Ground States, Transition Structures* (TS), *and Intermediates for the Rearrangement of s*-gauche-***1*** *to* cis-***8*** (*Fig. 1*). Basis sets: (U)B3LYP/6-31 G* (DFT1) and (U)M05-2X/6-311 + G** (DFT2); all energies in kcal mol^{-1} relative to s-*trans*-**1** (= 0.0 kcal mol^{-1}).

Structure	ΔE_{SCF} DFT1-Optimized	ΔE_{SCF} DFT2 Single point	ΔE_{SCF} DFT2-Optimized	ΔG DFT2	Distance of reacting centers [Å]
s-*trans*-**1**	0.0	0.0	0.0	0.0	1.521
s-*trans*-**1T**	0.3	– 0.3	– 0.3	0.3	1.534
s-*gauche*-**1**	2.5	2.1	2.0	2.5	1.519
s-*gauche*-**1T**	2.6	1.8	1.6	2.9	1.533
TS (s-*trans*-**1** → s-*trans*-**1T**)	1.0	1.1	1.2	1.6	1.534
TS (s-*gauche*-**1** → s-*gauche*-**1T**)	3.5	3.5	3.5	–	1.541
TS **2**, (s-*trans*-**1** → s-*gauche*-**1**)	3.5	3.3	3.5	–	1.513
TS **2**, (s-*trans*-**1** → s-*gauche*-**1T**)	4.2	3.7	3.8	–	1.522
TS **3**, (s-*gauche*-**1** → *endo,exo*-**4**)	23.0	30.1	30.4	29.1	2.217
endo,exo-**4**	21.9	28.9	29.1	28.1	2.425[a]) *r*(C(1)–C(5))
TS 5 (*endo,exo*-**4** → *endo,exo*-**6**)	25.4	32.3	32.4	–	3.729
endo,exo-**6**	25.0	30.9	30.9	30.5	3.104
TS *cis*-**7**	30.6	32.9	32.8	32.8	2.750
TS *trans*-**7**	36.5	38.5	–	–	–
cis-**8**	– 4.5	– 13.4	– 13.7	– 9.5	1.580
TS (*cis*-**8** → *trans*-**8**)	– 2.3	– 10.1	– 10.3	– 4.9	1.607
trans-**8**	– 4.6	– 13.0	– 13.5	– 8.9	1.576

[a]) Bond fixation for evaluation of **N**.

could not be calculated. The conformation s-*cis*-**1** suffers from steric strain and does not appear as an energy minimum in the calculation.

Before proceeding to the possible formation of intermediates, the structure of the final product, 3,4,4-triphenylcyclopent-1-ene (*cis*-**8**) will be described (*Scheme 2*). A cyclopentene ring is puckered [22], even more so than the envelope conformation of cyclopentane. The 3,4,4-triphenylcyclopent-1-ene contains – besides the (*Z*)-C=C bond – two stereoelements, the tetrahedral C(3) and the flap of the envelope, *i.e.*, C(4),

Scheme 2

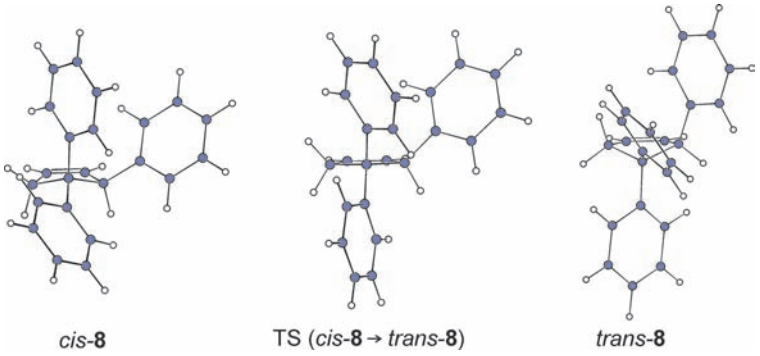

which can be *cis*- or *trans*-oriented to the 3-Ph group. The transition from *cis*-**8** to *trans*-**8** takes place *via* a planar cyclopentene (TS (*cis*-**8** → *trans*-**8**)) ring which was characterized as a true TS, showing only one negative vibrational frequency. This vibration connects the two conformations.

Energy values, all relative to the arbitrary zero point of 0.0 kcal mol^{-1} for s-*trans*-**1**, are collected in *Table 2*. The B3LYP/6-31G* calculation of ΔE_{SCF} places *cis*-**8** only 4.5 kcal mol^{-1} below s-*trans*-**1**, thus not describing the experimental situation properly. As is known from comparative studies on a set of model molecules, the B3LYP functional often fails to reproduce experimental energies [23]. It was this failure which led us to test other functionals of which *Truhlar*'s M05-2X/6-311 + G** (DFT2) proved to provide the best results [17]. Molecule *cis*-**8** is now by − 13.7 kcal mol^{-1} (ΔE_{SCF}) and − 9.5 kcal mol^{-1} (ΔG) below s-*trans*-**1**. The ΔG energy of *trans*-**8** is by 0.6 kcal mol^{-1} above that of *cis*-**8**, and a barrier of 4.0 kcal mol^{-1} (ΔG) has to be passed for the conversion (see *Table 2*).

Interestingly, the X-ray-analysis of **8** [15] revealed two crystallographically independent conformations, both of which are *trans*-***8***. Possibly, packing forces in the crystal overcompensate the small calculated difference in ΔG of *cis*-**8** and *trans*-**8**.

3.2. *Potential-Energy Surface for the Rearrangement of s*-gauche-**1** *with Intermediates.* The TSs of rearrangement (*cis*-**7** → *cis*-**8** and *trans*-**7** → *trans*-**8**) are the highest points of the energy profile. Reversible ring opening of s-*trans*-**1** gives biradical *exo*,*exo*-**4** (*Scheme 3*) which cannot cyclize to **8**, as will be discussed in *Sect. 3.4*; the prefixes *endo* and *exo* characterize the orientations of the substituents of the allylic radical system. *Fig. 1* shows the potential-energy surface and simulates the reaction course. The cleavage of the bond C(1)–C(2) of the cyclopropane is promoted by the stabilizing effects of three Ph groups. The ring opening of s-*gauche*-**1** leads *via* TS **3** ($\Delta G =$ + 29.1 kcal mol^{-1}) to an intermediate biradical *endo*,*exo*-**4** ($\Delta G =$ + 28.1 kcal mol^{-1}); the potential-energy trough is only 1.0 kcal mol^{-1} (ΔG) deep, but lends *endo*,*exo*-**4** the character of a true intermediate. The two Ph groups at C(1) adjust, as shown in formula *endo*,*exo*-**4** (*Scheme 3*, lower line).

The conversion to TS *cis*-**7** for rearrangement requires comment. According to the calculation, the bond system at Ph_2CH radical center C(1) is completely planar, and the 1,4-positions of the twisted Ph groups remain in that plane. In the minimum-energy conformation of *endo*,*exo*-**4** shown in *Scheme 3*, the distance of radical centers C(1) and C(5) (3.57 Å) is too large for direct bonding interaction. An approach succeeds by rotations about single bonds which are energetically not demanding (conformational change). To our surprise, a conformer *endo*,*exo*-**6** occurs as an intermediate which is by $\Delta G =$ 2.4 kcal mol^{-1} higher than *endo*,*exo*-**4**. A barrier TS **5** with ΔE_{SCF} of 3.3 kcal mol^{-1} has to be overcome in the conversion *endo*,*exo*-**4** → *endo*,*exo*-**6**. This new intermediate is well secured by ΔE_{SCF} barriers, 1.5 kcal mol^{-1} (TS **5**) *vs.* *endo*,*exo*-**3**, and 1.9 kcal mol^{-1} (TS **7**) toward *cis*-**8**. The distance of C(1) and C(5) has shrunk to 3.10 Å in *endo*,*exo*-**6** (*Scheme 4*).

The potential-energy surface is still rather flat, but involves discrete intermediates and TSs (*Fig.1*). In contrast, the computational results by *Houk et al.* [6] for the unsubstituted vinylcyclopropane furnished a flat surface without energy wells. Here, TSs and intermediates are fully characterized as being either maxima or minima with one negative or only positive vibrational frequencies, respectively. Biradical *endo*,*exo*-**4**

Scheme 3

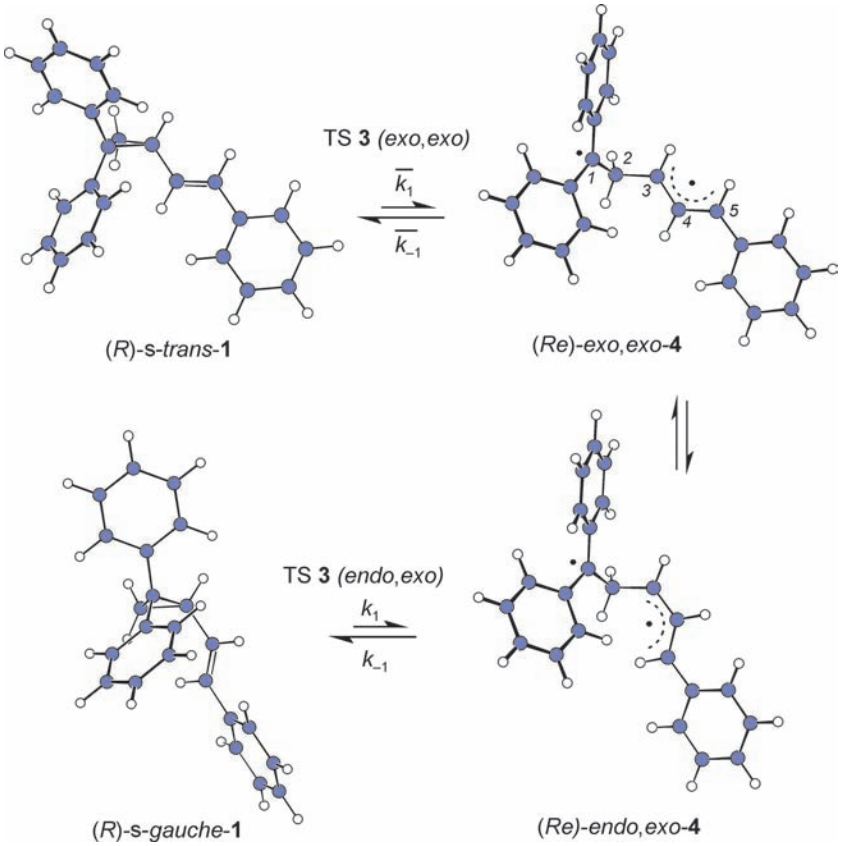

shows an $\langle S^2 \rangle$ value of 1.02. The biradical character according to CAS(4,4)/6-31G* single-point calculations on the B3LYP/6-31G* structure is 58% for *endo*,*exo*-**4**. TS *cis*-**7** shows structural similarities to the unsubstituted example (*Scheme 4*) [6], only

Scheme 4

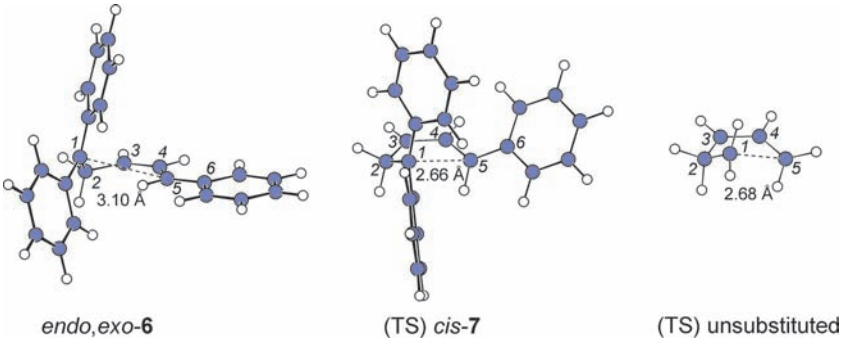

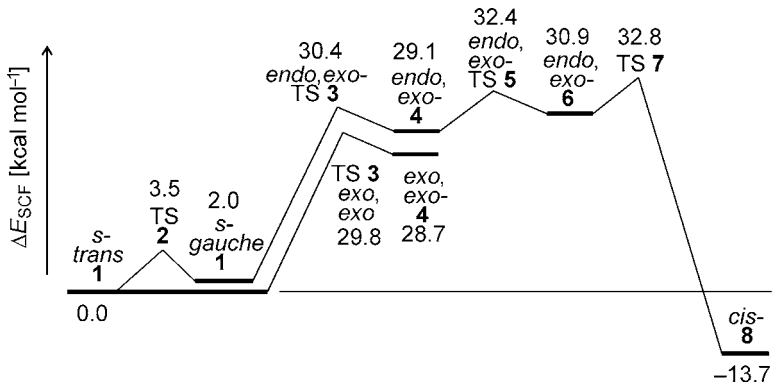

Fig. 1. *Potential-energy surface* (ΔE_{SCF}) *for the rearrangement of s*-trans-**1** via *s*-gauche-**1** *to* cis-**8** *with intermediates*

slightly distorted by the presence of the Ph groups. In *cis*-**7**, the centers which react to form the five-membered ring are separated by 2.66 Å, whereas this distance amounts to 2.68 Å for the unsubstituted case. The Ph group at C(5) of the TS *cis*-**7** is no longer in the plane of the allylic radical, but has a partial benzyl radical character. The motions require energy which is partially compensated by the gain in benzylic resonance energy.

It can be concluded that the potential-energy surface is lowered compared to that of the unsubstituted vinylcyclopropane, due to three conjugated Ph groups. However, the energy surface of the triphenyl derivative is structured, and, according to our expectations, intermediates and TSs are found. In the next section, water will be shed into the wine.

3.3. *Potential-Energy Surface for the Rearrangement of s*-gauche-**1** *without Intermediates.* As described above, the bond system of C(1) is planar, and the *geminal* phenyl groups reside with their 1,4-axes in that plane, but assume discrete twist angles about these 1,4-axes in their stable conformations. *Scheme 3* shows the conformations s-*trans*-**1** and s-*gauche*-**1** on ring opening to give rise to *exo*,*exo*-**4** and *endo*,*exo*-**4**. In the latter, the twist angles of geminal phenyl groups, *cis*- and *trans*-oriented to styryl, amount to $+32.1$ and $-21.6°$, respectively (*Sect. 3.6.2*). When these twist angles were more or less exchanged, it came as a surprise, that *endo*,*exo*-**4N** was *not a stationary point* on the potential-energy surface. In searching for a local energy minimum, *endo*,*exo*-**4N** fell back to s-*trans*-**1**. On the way up, the TS *cis*-**7N** was reached without passing any local minimum.

Fig. 2 describes the potential-energy surface for this geminal diphenyl conformation which we termed **N** for non-stationary. The resemblance with the behavior of the unsubstituted vinylcyclopropane [6] is obvious. Indeed, *endo*,*exo*-**4N** could be calculated only when fixing the C(1)–C(3) distance to 2.425 Å, the value in the *intermediate endo*,*exo*-**4**. In the conversion *endo*,*exo*-**4** → *endo*,*exo*-**4N**, a barrier of 1.5 kcal mol^{-1} in ΔE_{SCF} has to be passed, and **4N** is located by 0.9 kcal mol^{-1} below **4**. One may speak of a protection wall between the energy profiles *with* and *without* intermediates. The rotational angles of geminal diphenyl groups will be discussed in *Sect. 3.6.2.*

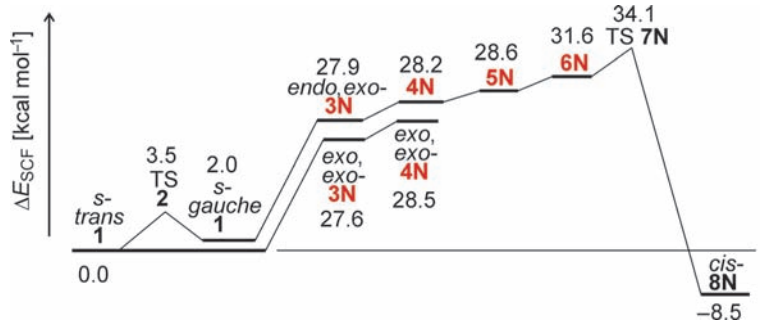

Fig. 2. *Potential-energy surface* (ΔE_{SCF}) *for the rearrangement of s*-trans-**1** via *s*-gauche-**1** *to* cis-**8** *without intermediates*

The reason for the observation of *endo*,*exo*-**4** as intermediate may not be due to a difference in the electronic stabilization of the biradical, but other effects could be responsible for leading to a small energy minimum for *endo*,*exo*-**4** but not for *endo*,*exo*-**4N**. A closer look at the space-filling models (*Scheme 5*) provides a possible explanation. A steric hindrance in *endo*,*exo*-**4** might be present at the position indicated by the arrow in the model which could cause the minimum for *endo*,*exo*-**4**. The formulae in the lower part of *Scheme 5* present the spin distribution; the C-atom of

Scheme 5

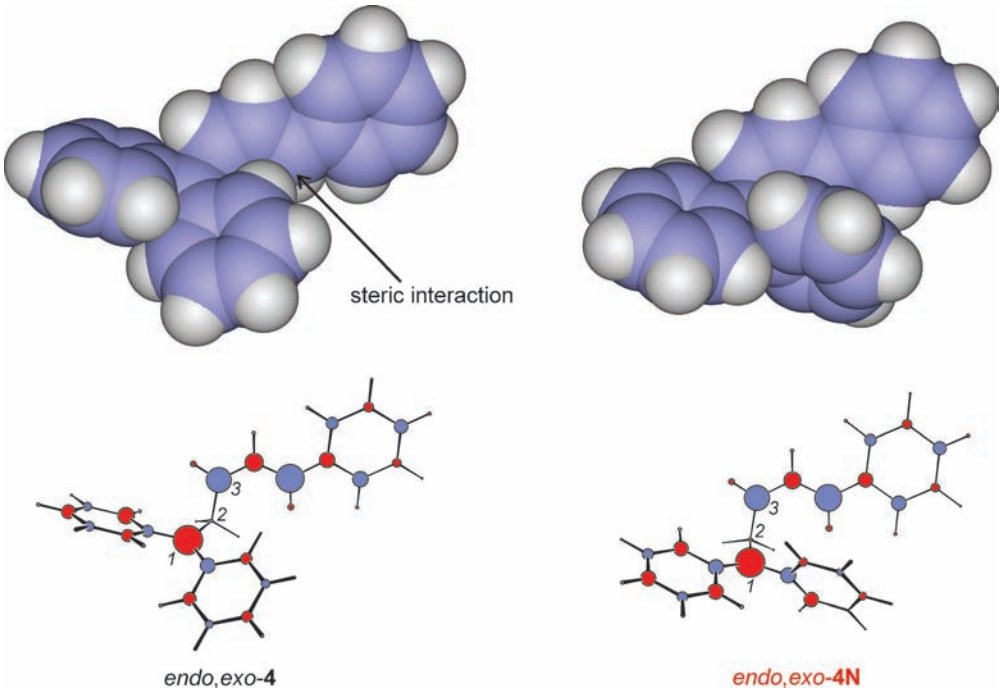

the Ph_2CH part and the allylic part carry most of the diradical character, whereas the three Ph groups contribute less.

For continuity of the structural changes, the suffix **N** is retained in the TS *cis*-**7N** of cyclization which is still different from TS *cis*-**7**. The ring closure leads to the stable cyclopentene **8N**. The energy values compiled in *Table 3* are obtained from the structures without the supplement **N** by bond fixation, as described above. *Scheme 6* displays transition structures and corresponding cyclization products **8** for different conformations of the cyclopentene ring. With ΔE_{SCF} of 32.8 kcal mol^{-1}, TS *cis*-**7** is the lowest pass for cyclization, and TS *cis*-**7N** is by 1.4 kcal mol^{-1} higher. The TS *trans*-**7** ($\Delta E_{SCF} = 38.5$ kcal mol^{-1}) is listed only for completeness.

Table 3. *Energies of Ground States, Transition Structures* (TS), *and Intermediates for the Rearrangement of s*-gauche-***1*** *to* cis-***8*** (*Fig. 1*). Basis sets: (U)B3LYP/6-31 G* (DFT1) and (U)M05-2X/6-311 + G** (DFT2); all energies in kcal mol^{-1} relative to s-*trans*-**1** (= 0.0 kcal mol^{-1}).

Structure	ΔE_{SCF} DFT1-Optimized	ΔE_{SCF} DFT2 Single point	ΔE_{SCF} DFT2-Optimized	ΔG DFT2	Distance of reacting centers [Å]
s-*trans*-**1**	0.0	0.0	0.0	0.0	1.521
s-*gauche*-**1**	2.5	2.1	2.0	2.5	1.519
endo,*exo*-**3N**	21.0	27.6	26.9	–	2.217[a])
TS (*endo*,*exo*-**4** → *endo*,*exo*-**4N**)	23.9	30.4	30.6	–	2.378
endo,*exo*-**4N**	21.8	29.0	28.2	–	2.425[a])
					r(C(2)–C(5))
endo,*exo*-**5N**	22.7	30.2	28.6	–	3.638[b])
endo,*exo*-**6N**	26.1	31.1	31.6	–	3.104
TS *cis*-**7N**	31.0	34.2	34.1	34.5	2.706
TS *trans*-**7N**	35.1	36.9	–	–	–
cis-**8N**	– 0.4	– 8.3	– 8.5	– 3.9	1.579
trans-**8N**	– 1.7	– 10.1	– 10.4	– 5.5	1.598

[a]) Bond fixation for evaluation of **N**. [b]) The angle C(2)–C(1)–C(3) was fixed at 109.1°. This value is taken from TS **5**.

3.4. *Potential-Energy Surface for the Ring Opening of s*-trans-**1**. The reversible opening of the three-membered ring leads from s-*trans*-**1** to the biradical *exo*,*exo*-**4** (*Scheme 3*). The closure of the five-membered ring would require a preceding isomerization *exo*,*exo*-**4** → *endo*,*exo*-**4** with sacrifice of the allylic resonance energy (*ca.* 12 kcal mol^{-1}) [24]. The *endo*-attachment of the $Ph_2\dot{C}CH_2$ radical at C(3) of the allylic radical is mandatory for the formation of the cyclopentene derivative. The thermal equilibration of s-*trans*-**1** with *exo*,*exo*-**4** becomes visible by combination with racemization (*Sect. 3.5*) or by change of the *gem*-diphenyl conformation giving rise to *exo*,*exo*-**4N** (*Sect. 3.6*).

The ΔG values for the formation from s-*trans*-**1** show that the intermediate *exo*,*exo*-**4** (27.1 kcal mol^{-1}; *Table 4*) is slightly favored over *endo*,*exo*-**4** (28.1 kcal mol^{-1}). The TSs of ring opening differ more: $\Delta E_{SCF} = 29.8$ kcal mol^{-1} for TS **3** (s-*trans*-**1** → *exo*,*exo*-**4**) and 32.4 kcal mol^{-1} for TS (s-*trans*-**1** → *endo*,*exo*-**4**); that is an advantage of 2.6 kcal mol^{-1} in the racemization of the enantiomers of s-*trans*-**1** (*Sect. 3.5*).

Table 4. *Energies for Ring Opening of s*-trans-**1** *to* exo,exo-**4** *and* exo,exo-**4N**, *and Energies of Ground States, Transition Structures* (TS), *and Intermediates for the Rearrangement of s*-gauche-**1** *to* cis-**8** (*Figs. 1* and *2*). Basis sets: (U)B3LYP/6-31 G* (DFT1) and (U)M05-2X/6-311 + G** (DFT2); all energies in kcal mol^{-1} relative to s-*trans*-**1** (= 0.0 kcal mol^{-1}).

Structure	ΔE_{SCF} DFT1-Optimized	ΔE_{SCF} DFT2 Single point	ΔE_{SCF} DFT2-Optimized	ΔG DFT2	Distance of reacting centers [Å]
s-*trans*-**1**	0.0	0.0	0.0	0.0	1.521
TS **3** (s-*trans*-**1** → *exo*,*exo*-**4**)	21.4	29.4	29.8	–	2.200
exo,*exo*-**4**	20.6	28.4	28.7	27.1	2.430
TS (*exo*,*exo*-**4** → *exo*,*exo*-**4N**)	22.2	29.4	29.8	29.4	2.345
TS (s-*trans*-**1** → *exo*,*exo*-**4N**)	19.8	27.5	27.6	–	2.200[a])
exo,*exo*-**4N**	20.5	28.5	28.5	–	2.430[a])
					r(C(1)–C(5))
endo,*exo*-**4**	21.9	28.9	29.1	28.1	2.425
TS ((*re*)-*endo*,*exo*-**4** → (*si*)-*endo*,*exo*-**4**)	23.0 (A)[b])	29.9	30.3	–	4.438
	26.1 (B)[b])	32.4	–	–	–
exo,*exo*-**4**	20.6	28.4	28.7	27.1	2.430
TS ((*re*)-*exo*,*exo*-**4** → (*si*)-*exo*,*exo*-**4**)	22.7 (A)[b])	30.4	–	–	–
	22.8 (B)[b])	30.0	–	–	–

[a]) Bond fixation for the evaluation of **N**. [b]) See *Scheme 7*.

The ΔE_{SCF} value of 28.5 kcal mol^{-1} for the non-stationary *exo*,*exo*-**4N** is virtually the same as for the intermediate *exo*,*exo*-**4** (28.7 kcal mol^{-1}), but the TS of conversion is by 1.1 kcal mol^{-1} higher.

3.5. *Racemization of Optically Active* **1**. Faster than the ring expansion yielding *cis*-**8** is the racemization of the enantiomers of **1**. How does that occur? When s-*gauche*-**1** opens the three-membered ring and furnishes *endo*,*exo*-**4**, a TS *endo*,*exo*-**3** is passed in which the bond system of C(1), the incipient $Ph_2\dot{C}$ radical center, as well as that of the allylic group has almost reached planarity, In the course of this ring opening, the chirality of (*R*)-**1** and (*S*)-**1** survives in the biradicals and is expressed by the descriptors *Re* and *Si* of two-dimensional chirality (*Scheme 3*). The loss of stereochemical integrity occurs in a rotation about the bond C(2)–C(3). The phenylallyl group swings around and passes a *quasi*-orthogonal state of the two parts of the biradical. Both conformations of **1** can participate in the process which is formally dissected in three steps:

$$(R)\text{-s-}gauche\text{-}\mathbf{1} \rightleftharpoons (Re)\text{-}endo,exo\text{-}\mathbf{4} \rightleftharpoons (Si)\text{-}endo,exo\text{-}\mathbf{4} \rightleftharpoons (S)\text{-s-}gauche\text{-}\mathbf{1}$$

$$(R)\text{-s-}trans\text{-}\mathbf{1} \rightleftharpoons (Re)\text{-}exo,exo\text{-}\mathbf{4} \rightleftharpoons (Si)\text{-}exo,exo\text{-}\mathbf{4} \rightleftharpoons (S)\text{-s-}trans\text{-}\mathbf{1}$$

The interconversion $(Re) \rightleftharpoons (Si)$ requires an activation energy ΔE_{SCF} amounting to 1.0 kcal mol^{-1} for *endo*,*exo*-**4** and 2.0 kcal mol^{-1} for *exo*,*exo*-**4** (*Table 4*). Starting from the global energy minimum of s-*trans*-**1**, the racemization barrier is reached at ΔE_{SCF} of 29.9 kcal mol^{-1} for the pathway *via endo*,*exo*-**4** and 30.4 kcal mol^{-1} for *exo*,*exo*-**4** as an intermediate. That suggests a preference of the pathway *via endo*,*exo*-**4**, but the difference of 0.5 kcal mol^{-1} is too small to be trusted, the less so, as structural optimization failed in one of the two TSs.

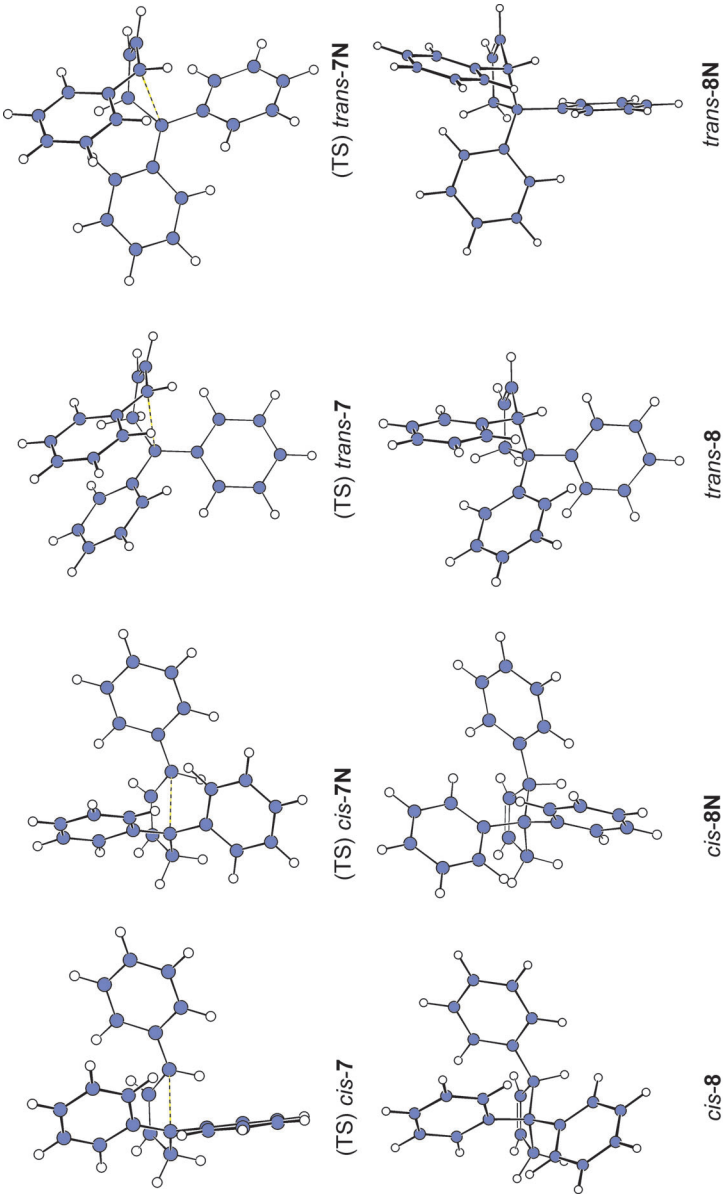
(TS) trans-7N
trans-8N
(TS) trans-7
trans-8
(TS) cis-7N
cis-8N
(TS) cis-7
cis-8

Scheme 6

A closer look reveals that there are two directions for the rotation about the bond C(2)–C(3) in the interconversion (*Re*) ⇌ (*Si*). In *Pathway a* of *Scheme 7*, only the H-atom at C(3) 'sticks down' and interferes with the upper half of the biradical. On *Path b*, the entire phenylallyl radical stays 'down' and has to pass by the $Ph_2\dot{C}$ radical. The sterically more demanding process *b* suffers from a higher activation energy (*Table 4*), mainly in the case of *endo*,*exo*-**4**.

Scheme 7

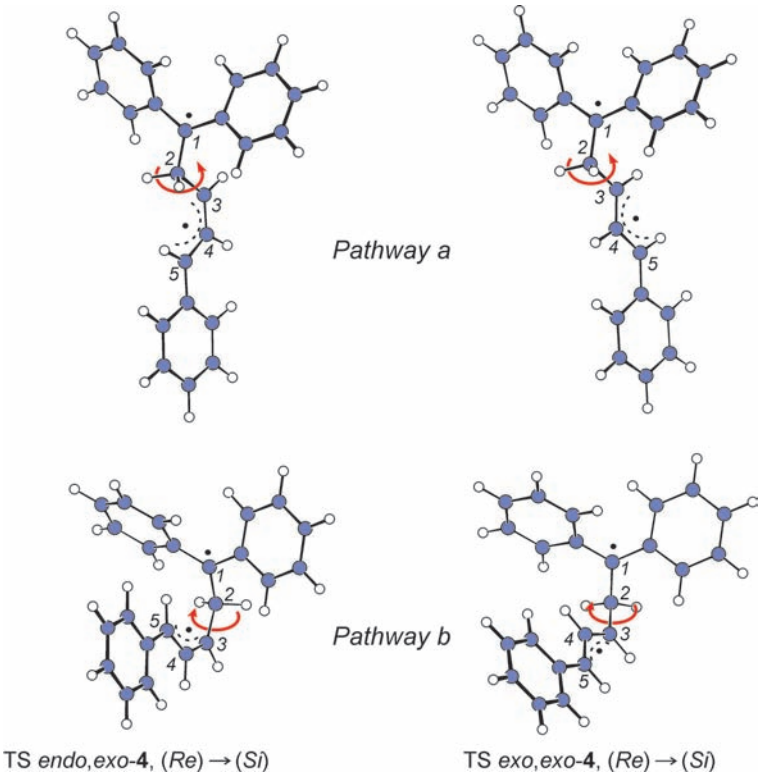

As pointed out in *Sect. 3.4*, the ring opening of s-*trans*-**1** is a dead-end road allowing racemization, but no cyclopentene formation. The reaction *via* s-*gauche*-**1** and *endo*,*exo*-**4** reaches the TS(*cis*-**7** → *cis*-**8**) of ring expansion at ΔE_{SCF} (opt.) of 32.8 kcal mol^{-1}, *i.e.*, 2.5 kcal mol^{-1} above the barrier of racemization. The experimental $\Delta G^{\#}$ (100°) favors racemization by 3.9 kcal mol^{-1} [15].

3.6. *Conformational Changes of Geminal Diphenyl Groups.* 3.6.1. *At Tetrahedral C-Atom.* Stationary and non-stationary biradicals (*Sects. 3.2* and *3.3*) differ only in the conformations of the geminal diphenyl group. Thus, learning about the Ph flipping and the angles of twist arouses interest. In the process of energy optimization, the position of one Ph group was rotated by a certain value, while the second Ph group was allowed

to find the conformation of lowest energy. In this way, the energy profile of the coupled geminal diphenyl rotation was amenable, but the flatness near the minimum reduced precision. Numerical values of twist angles must be clearly defined *vs.* a zero standard. The CBS-QB3 method, in general, provides the best energy values, but is restricted to smaller molecules. Therefore, the optimized functional MO5-2X/6-311 + G** was applied here.

In diphenylmethane (**9**), the simplest model for the Ph_2C group, the twist angles of geminal diphenyl are determined *vs.* their coplanar arrangement with the plane C(2)–C(1)–C(4) as zero standard. The dihedral angles C(3)C(2)–C(1)C(4) and C(2)C(1)–C(4)C(5) are the angles of Ph twist which are measured by viewing along the bond axes C(2)–C(1) and C(4)–C(1). In the ground-state of **9**, rotation angles of $+51°$ and $+51°$ are found (*Table 5*, below); the identity and the same sign establish C_2 symmetry (*Scheme 8*). In the TS of Ph flipping, twist angles of 90° and 0° characterize T-stacking. The central angle C(2)–C(1)–C(4) of 114.8° in **9** is widened to 116.3° in **9T**.

Scheme 8

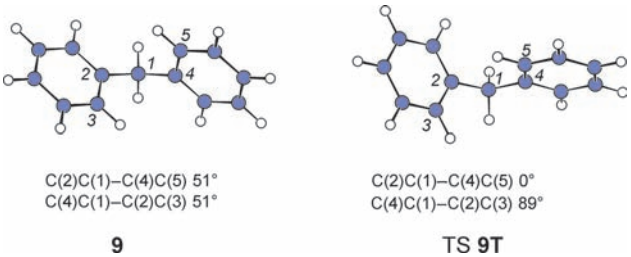

A step closer to structure **1** is 1,1-diphenylcyclopropane (**10**). Its ground-state has a V structure with twist angles of 89° and 90°, suggesting C_{2v} symmetry. The T-stacked conformation is by ΔG of 1.8 kcal mol^{-1} above the ground state, and torsion angles of 89° and 0° confirm the orthogonality. In contrast to **9** and **9T**, however, a barrier of ΔG of 3.4 kcal mol^{-1} separates **10** and **10T**, *i.e.*, **10T** I is a true *intermediate* in the Ph flipping. With the exception of the T-stacked structures, all compounds and TSs of *Table 5* show a propeller-like arrangement of the geminal phenyl groups. As a consequence, both twist angles have the same sign (+ + or − −); thus no statements of sign are required in *Table 5*.

The introduction of an (*E*)-2-phenylethenyl group into the three-membered ring of **10** makes the geminal phenyl groups in **1** different, their twist angles, α(*cis*) and α(*trans*) included; **1** occurs in enantiomers [15]. The *trans*-Ph group has more rotational freedom than *cis*-Ph, and α(*trans*) is larger than α(*cis*) in s-*trans*-**1** and s-*gauche*-**1** (*Table 5* and *Scheme 3*). In the calculated stacked s-*trans*-**1T**, the *trans*-Ph ($\alpha = 1°$) lies in the bisectorial plane of C(2), and α(*cis*) of 81° comes close to orthogonality. The crystal packing in **1T** (X-ray) leads to a certain deformation.

3.6.2. *Conformation of Diphenylmethyl in Open-Chain Biradical.* The calculation indicates planarity for the bond system of C(1), the center of the $Ph_2\dot{C}$ radical. The twist angles of geminal diphenyl are defined *vs.* the coplanar arrangement of $Ph_2C(1)$ as zero value; the view from the Ph groups to C(1) determines the sign.

Table 5. *Calculated* (M05-2X/6-311 + G**) *Energies and Twist Angles of* Geminal *Diphenyl Groups at Tetrahedral C-Atom*

	ΔE_{SCF} [kcal mol^{-1}]	ΔG [kcal mol^{-1}]	Twist Angles [°]	
			α_1	α_2
Diphenylmethane (**9**)	0.0	0.0	51	51
TS **9T**	0.3	0.3	89	0
1,1-Diphenylcyclopropane (**10**)	0.0	0.0	89	90
TS (**10** → **10T**)	0.5	3.4	72	43
10T	−0.7	1.8	89	0.0
			α(*cis*)	α(*trans*)
s-*trans*-**1**	0.0	0.0	73	80
TS **2** (s-*trans*-**1** → s-*gauche*-**1**)	3.5	[a])	59	72
s-*gauche*-**1**	2.1	2.5	68	75
s-*trans*-**1T**	−0.3	0.3	81	0.8
1T (X-Ray)			85	15
TS (s-*trans*-**1** → s-*trans*-**1T**)	1.1	1.6	90	41

[a]) Convergence criteria not fulfilled (*Sect. 2*).

As in **1**, the geminal Ph groups in the open-chain biradicals are structurally different, *cis*- and *trans*-oriented to the phenylallyl group. Benzyl resonance and steric hindrance compete in establishing the angles of twist. In (*Re*)-exo,*exo*-**4** steric interaction increases the angle of *cis*-Ph to −35°, compared with −20° for *trans*-Ph (*Scheme 9*). According to *Table 6*, the three intermediates, *i.e.*, *endo*,*exo*-**4**, *endo*,*exo*-**6**, and *exo*,*exo*-**4**, show nearly identical pairs of twist angles. Thus, the conformation of $Ph_2C(1)$ hardly responds to the *endo*- or *exo*-attachment at the allylic radical. The dominance of the propeller-type overlap of the geminal Ph groups is shown by the same direction of twist. In *Table 6*, the signs are important; values of >90° are expressed as (180 − α)° with change of sign.

Scheme 9

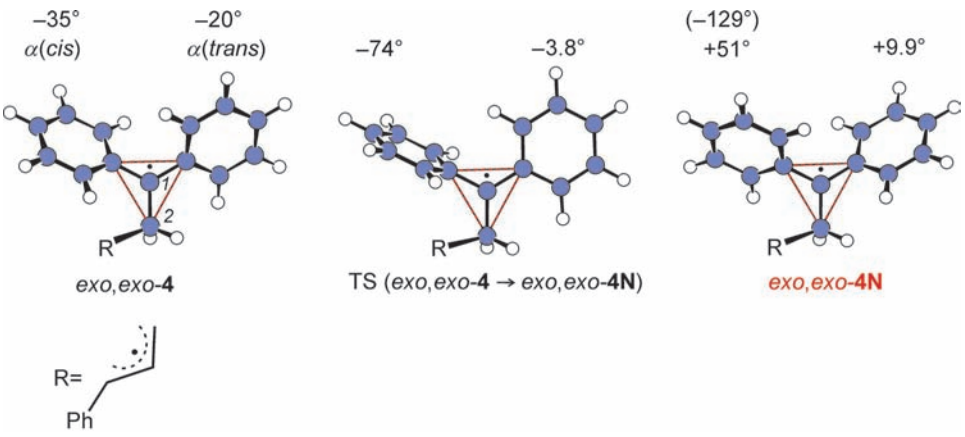

Table 6. *Calculated (*Re*)-Biradical Conformations* (M05-2X/6-311 + G**)*: Twist Angles* α [°] *of Geminal Diphenyl Groups* vs. *Bond Plane of C(1)*

Formula (*Figs. 1* and *2*)	Stationary: I, TS		Nonstationary: **N**	
	cis-Ph	*trans*-Ph	*cis*-Ph	*trans*-Ph
TS **3** (s-*gauche*-**1** → *endo*,*exo*-**4**)	−7.7	−51	+61	+4.7
endo,*exo*-**4**	−32	−22	+64	+3.6
TS (*endo*,*exo*-**4** → *endo*,*exo*-**4N**)	−73	−3.2		
TS **5** (*endo*,*exo*-**4** → *endo*,*exo*-**6**)	−5.7	−51	+64	+4.0
endo,*exo*-**6**	−33	−23	+40	+16
TS **7** (*endo*,*exo*-**6** → *cis*-**8**)	−33	−21		
TS **3** (s-*trans*-**1** → *exo*,*exo*-**4**)	−11	−47	+60	+5.3
exo,*exo*-**4**	−35	−20	+51	+9.9
TS (*exo*,*exo*-**4** → *exo*,*exo*-**4N**)	−74	−3.8		

The central step of the racemization is the equilibration (*Re*) ⇌ (*Si*). In this process, the rotation about the bond C(2)–C(3) is synchronized with the flipping of the geminal Ph groups by which the twist angles are exchanged; those of (*Re*) and (*Si*) differ in sign.

The calculations revealed a second energy profile for the conversion of **1** to **8** which lacks intermediates (*Sect. 3.3*, *Fig. 2*). Only by freezing of one bond distance, the non-stationary structures became amenable to calculation. *Scheme 9* discloses the change in twist direction during the conversion of *exo*,*exo*-**4** to give *exo*,*exo*-**4N** and likewise includes the TS for Ph flipping. In the conversion of *exo*,*exo*-**4** to *exo*,*exo*-**4N**, the twist angle α(*cis*) changes from −35° *via* −74° to −129° (= +51°), *i.e.*, by a total of 94°, while α(*trans*) flips only by 30°. The *trans*-Ph group in the TS is nearly coplanar with the C(1) bond plane, whereas the *cis*-Ph approaches the orthogonal position. Thus, a flipping mechanism related to T-stacking is preferred over the passing of the coplanar conformation (0°/0°). According to the energies ΔE_{SCF} (*Table 4*), the TS is located by 1.1 kcal mol^{-1} above *exo*,*exo*-**4** and 1.3 kcal mol^{-1} above *exo*,*exo*-**4N**.

The Ph twist angles of the **N** series are quite different from those of the stationary structures, but present only marginal differences among themselves (*Table 6*).

REFERENCES

[1] E. Vogel, *Angew. Chem.* **1960**, *72*, 27.
[2] C. G. Overberger, A. E. Borchert, *J. Am. Chem. Soc.* **1960**, *82*, 1007.
[3] R. B. Woodward, R. Hoffmann, *Angew. Chem., Int. Ed.* **1969**, *8*, 781.
[4] W. v. E. Doering, W. R. Roth, *Angew. Chem., Int. Ed.* **1963**, *2*, 115.
[5] W. v. E. Doering, W. R. Roth, *Tetrahedron* **1963**, *19*, 715.
[6] K. N. Houk, M. Nendel, O. Wiest, J. W. Storer, *J. Am. Chem. Soc.* **1997**, *119*, 10545.
[7] E. R. Davidson, J. J. Gajewski, *J. Am. Chem. Soc.* **1997**, *119*, 10543.
[8] J. E. Baldwin, *Chem. Rev.* **2003**, *103*, 1197.
[9] M. Nendel, D. Sperling, O. Wiest, K. N. Houk, *J. Org. Chem.* **2000**, *65*, 3259.
[10] C. Doubleday Jr., M. Nendel, K. N. Houk, D. Thweatt, M. Page, *J. Am. Chem. Soc.* **1999**, *121*, 4720.
[11] C. Doubleday Jr., G. S. Li, W. L. Hase, *Phys. Chem. Chem. Phys.* **2002**, *4*, 304.
[12] B. K. Carpenter, *Annu. Rev. Phys. Chem.* **2005**, *56*, 57.

[13] J. E. Baldwin, S. Bonacorsi, *J. Am. Chem. Soc.* **1993**, *115*, 10621.
[14] L. A. Asuncion, J. E. Baldwin, *J. Am. Chem. Soc.* **1995**, *117*, 10672.
[15] J. Mulzer, R. Huisgen, V. Arion, R. Sustmann, *Helv. Chim. Acta* **2011**, *94*, doi: 10.1002/hlca.201100135.
[16] Gaussian 03, Revision C.02, M. J. Frisch, G. W. Trucks, H. B. Schlegel, G. E. Scuseria, M. A. Robb, J. R. Cheeseman, J. A. Montgomery Jr., T. Vreven, K. N. Kudin, J. C. Burant, J. M. Millam, S. S. Iyengar, J. Tomasi, V. Barone, B. Mennucci, M. Cossi, G. Scalmani, N. Rega, G. A. Petersson, H. Nakatsuji, M. Hada, M. Ehara, K. Toyota, R. Fukuda, J. Hasegawa, M. Ishida, T. Nakajima, Y. Honda, O. Kitao, H. Nakai, M. Klene, X. Li, J. E. Knox, H. P. Hratchian, J. B. Cross, C. Adamo, J. Jaramillo, R. Gomperts, R. E. Stratmann, O. Yazyev, A. J. Austin, R. Cammi, C. Pomelli, J. W. Ochterski, P. Y. Ayala, K. Morokuma, G. A. Voth, P. Salvador, J. J. Dannenberg, V. G. Zakrzewski, S. Dapprich, A. D. Daniels, M. C. Strain, O. Farkas, D. K. Malick, A. D. Rabuck, K. Raghavachari, J. B. Foresman, J. V. Ortiz, Q. Cui, A. G. Baboul, S. Clifford, J. Cioslowski, B. B. Stefanov, G. Liu, A. Liashenko, P. Piskorz, I. Komaromi, R. L. Martin, D. J. Fox, T. Keith, M. A. Al-Laham, C. Y. Peng, A. Nanayakkara, M. Challacombe, P. M. W. Gill, B. Johnson, W. Chen, M. W. Wong, C. Gonzalez, J. A. Pople, *Gaussian*, *Inc.*, Wallingford, CT, 2004.
[17] Y. Zhao, N. E. Schultz, D. G. Truhlar, *J. Chem. Theory Comput.* **2006**, *2*, 364.
[18] S. V. Burley, G. A. Petsko, *Science* **1985**, *229*, 23.
[19] M. Nishio, H. Nishihata, *Tetrahedron* **1989**, *45*, 7201.
[20] K. C. Janda, J. C. Hemminger, J. S. Winn, S. E. Novick, S. J. Harris, W. Klemperer, *J. Chem. Phys.* **1975**, *63*, 1419.
[21] M. O. Sinnokrot, C. D. Sherril, *J. Chem. Phys. A* **2006**, *110*, 10656.
[22] P. Rademacher, 'Strukturen organischer Moleküle', VCH, Weinheim, 1987.
[23] M. D. Wodrich, C. Corminboeuf, P. R. Schreiner, A. A. Fokin, P. v. R. Schleyer, *Org. Lett.* **2007**, *9*, 1851
[24] H.-G. Korth, H. Trill, R. Sustmann, *J. Am. Chem. Soc.* **1981**, *103*, 4483.

Received April 8, 2011